Research Square

Preprints are preliminary reports that have not undergone peer review.
They should not be considered conclusive, used to inform clinical practice,
or referenced by the media as validated information.

Comparative Outcomes of 3D-Printed Porous Artificial Vertebral Bodies and Titanium Mesh Cages After Single-Level Anterior Cervical Corpectomy and Fusion for Cervical Spinal Stenosis With Hyperextension Injury: A Retrospective Cohort Study

Linyang Song
Qilu Hospital of Shandong University
Xin Xu
Affiliated 960th Hospital of PLA, Shandong Second Medical University
Guangjun Jiao
jiaoguangjun@sdu.edu.cn

Qilu Hospital of Shandong University

Research Article

Keywords: 3D printing, porous artificial vertebral body, titanium mesh cage, anterior cervical corpectomy and fusion, cervical spinal stenosis, hyperextension injury, subsidence, fusion

Posted Date: November 19th, 2026

DOI: https://doi.org/10.21203/rs.3.rs-11209081/v1

License: This work is licensed under a Creative Commons Attribution 4.0 International License.
Read Full License

Additional Declarations: No competing interests reported.

Abstract

Objective

To compare the perioperative, clinical, and radiographic outcomes of 3D-printed porous artificial vertebral bodies and titanium mesh cages (TMCs) for anterior column reconstruction after single-level anterior cervical corpectomy and fusion (ACCF) in patients with cervical spinal stenosis combined with hyperextension injury, and to identify factors associated with postoperative subsidence.

Methods

This single-center retrospective comparative cohort study included 140 consecutive patients who underwent single-level ACCF between 2023 and 2025, with 70 patients in the 3D group and 70 in the TMC group. Baseline characteristics, perioperative parameters, clinical outcomes, radiographic outcomes, and complications were compared between groups. The main radiographic outcomes included subsidence, reconstructed segmental height loss (ΔH), absolute change in the C2–7 sagittal vertical axis (ΔcSVA), loss of the C2–C7 Cobb angle, and fusion rates at 6 and 12 months. Multivariable logistic regression was used to identify factors associated with subsidence. Stabilized inverse probability of treatment weighting (IPTW) was additionally performed as a sensitivity analysis to address measured treatment-selection imbalance.

Results

The 3D group had a shorter operative time, less intraoperative blood loss, and a shorter hospital stay than the TMC group (all $P \leq 0.002$). The JOA recovery rate was higher in the 3D group (78.0 ± 13.8% vs 69.0 ± 14.3%, $P < 0.001$), whereas postoperative NDI was borderline different ($P = 0.050$) and VAS reduction was similar between groups ($P = 0.544$). The 3D group showed a lower subsidence rate than the TMC group (17.1% vs 61.4%, $P < 0.001$), less height loss (1.0 ± 0.6 vs 2.5 ± 0.9 mm, $P < 0.001$), a smaller absolute change in cSVA (11.6 ± 3.1 vs 22.0 ± 5.4 mm, $P < 0.001$), and less loss of the C2–C7 Cobb angle (1.0 ± 0.3° vs 3.1 ± 1.4°, $P < 0.001$). The 6-month fusion rate was higher in the 3D group (85.7% vs 40.0%, $P < 0.001$), whereas the 12-month fusion rates were similar (94.3% vs 88.6%, $P = 0.366$). Multivariable analysis showed that use of a 3D-printed vertebral body was associated with lower odds of subsidence (adjusted OR 0.035, 95% CI 0.010–0.116, $P < 0.001$). Each 10-HU decrease in the lower adjacent vertebral body (OR 1.189, 95% CI 1.096–1.291, $P < 0.001$) and each 1-mm increase in immediate postoperative reconstructed height (OR 1.417, 95% CI 1.090–1.840, $P = 0.009$) were associated with higher odds of subsidence. The IPTW sensitivity analysis yielded a directionally consistent association (OR 0.078, 95% CI 0.032–0.185, $P < 0.001$).

Conclusions

In patients with cervical spinal stenosis combined with hyperextension injury undergoing single-level ACCF, use of a 3D-printed porous artificial vertebral body was associated with lower postoperative subsidence, less radiographic change, and a higher early fusion rate than TMC reconstruction. The difference in fusion was no longer significant at 12 months, suggesting a potential benefit mainly in accelerating early fusion rather than increasing the ultimate likelihood of fusion. Lower adjacent vertebral HU values and greater immediate postoperative reconstructed height were also associated with higher odds of subsidence. Because of the retrospective nonrandomized design, these findings require further validation in prospective multicenter studies.

1. Introduction

- Cervical hyperextension injury frequently occurs in patients with pre-existing cervical spinal stenosis, degenerative cervical disease, or ossification of the posterior longitudinal ligament (OPLL). In these patients, hyperextension trauma may cause the spinal cord to be compressed between anterior and posterior structures within an already narrowed spinal canal, resulting in central cord syndrome or other forms of incomplete spinal cord injury [1]. For patients with prominent anterior compression, particularly when posterior vertebral osteophytes or OPLL substantially compromise the effective spinal canal, anterior direct decompression and reconstruction remain important surgical options [2, 3].
- Anterior cervical corpectomy and fusion (ACCF) enables direct removal of anterior compressive lesions while simultaneously restoring anterior column continuity and stability [2]. However, postoperative outcomes depend not only on adequate neural decompression but also on the mechanical stability of the implant–endplate interface and subsequent bony fusion. Implant subsidence remains an important radiographic complication after ACCF because it may be accompanied by loss of reconstructed segmental height, changes in cervical alignment, increased loading of the fixation construct, and impaired progression of fusion [4].
- Titanium mesh cages (TMCs) have been widely used for anterior column reconstruction because of their structural strength, technical familiarity, and broad availability. Nevertheless, conventional TMCs generally require intraoperative trimming and adaptation, and incomplete conformity between the cage and adjacent vertebral endplates may result in localized stress concentration and endplate damage [4]. In addition to implant-related factors, patient-specific bone quality and reconstruction technique may also influence subsidence. Lower computed tomography Hounsfield unit (HU) values of adjacent vertebral bodies have been associated with an increased risk of subsidence after ACCF [5]. Excessive intraoperative distraction, inappropriate cage length, and overcorrection of cervical alignment have also been reported as potential risk factors [6]. More recently, MRI-based vertebral bone quality measurements have been explored as additional tools for preoperative subsidence risk assessment [7].
- Three-dimensional (3D)-printed porous artificial vertebral bodies have been introduced as an alternative reconstruction option. Their designable porous architecture, relatively large implant–endplate contact surface, and potential for improved geometric conformity may contribute to more

favorable load distribution and interface stability, while the porous surface may facilitate bone ingrowth and osseointegration [8]. Previous comparative studies and meta-analyses have reported associations between 3D-printed vertebral bodies and lower subsidence, improved maintenance of reconstructed height, and favorable cervical sagittal parameters [9]. However, these findings have not been uniform across studies. Some reports have identified differences mainly in selected radiographic outcomes, whereas mid-term clinical outcomes have been broadly comparable between reconstruction strategies [10]. More recent propensity score-matched analyses have suggested that differences may be particularly evident in early fusion and selected radiographic maintenance parameters, while mid-term fusion, subsidence, and functional recovery may be similar in some cohorts [11]. A prospective nonrandomized comparison has likewise shown that the relative performance of different reconstruction materials may vary according to the specific outcome and clinical setting [12].

- Importantly, most existing comparative studies of 3D-printed vertebral bodies and TMCs have focused on patients with degenerative cervical myelopathy or OPLL. Evidence remains limited for patients with cervical spinal stenosis combined with hyperextension injury, in whom pre-existing degenerative narrowing and acute traumatic neurological injury coexist and stable anterior column reconstruction may be particularly relevant. Therefore, the present study compared the perioperative, clinical, radiographic, and complication outcomes of 3D-printed porous artificial vertebral bodies and conventional TMCs after single-level ACCF in this specific patient population. In addition, we explored factors associated with postoperative subsidence to further characterize potential determinants of reconstruction failure.

2 Materials and methods

2.1 Study design and patients

This was a single-center retrospective comparative cohort study. A total of 140 consecutive patients with cervical spinal stenosis combined with hyperextension injury who underwent single-level anterior cervical corpectomy and fusion (ACCF) with anterior column reconstruction at the Qilu Hospital of Shandong University, between 2023 and 2025 were included. Patients were divided according to the reconstruction implant into a 3D group and a titanium mesh cage (TMC) group, with 70 patients in each group. All patients completed at least 12 months of clinical and radiographic follow-up.

Both reconstruction techniques were available and used concurrently throughout the study period, and the 3D-printed vertebral body did not sequentially replace the TMC. Treatment allocation was not randomized. Implant selection was influenced primarily by patient preference and financial considerations because the 3D-printed vertebral body was more expensive than conventional TMC, while routine clinical and anatomical factors were also considered when necessary. To assess potential chronological imbalance, the annual distribution of cases from 2023 to 2025 was compared between groups (Supplementary Table S1).

The study was approved by the Ethics Committee of the Qilu Hospital of Shandong University (No. QLCR20260629). Because of the retrospective design and use of anonymized data, the requirement for written informed consent was waived in accordance with institutional requirements.

2.2 Inclusion and exclusion criteria

The inclusion criteria were: (1) acute traumatic neurological dysfunction consistent with cervical hyperextension injury; (2) preoperative CT or MRI confirming cervical spinal stenosis, with or without degenerative changes, posterior vertebral osteophytes, or ossification of the posterior longitudinal ligament; (3) treatment with single-level ACCF and reconstruction using either a 3D-printed porous artificial vertebral body or TMC; (4) complete preoperative, immediate postoperative, and follow-up clinical and radiographic data; and (5) follow-up of at least 12 months.

The exclusion criteria were: (1) tumor, infection, tuberculosis, or pathological fracture; (2) previous cervical spine surgery; (3) concomitant posterior fixation or other additional stabilizing procedures; (4) severe multiple trauma or other conditions affecting neurological assessment; and (5) missing key radiographic data precluding evaluation of subsidence, fusion, or major radiographic parameters.

2.3 Data collection

Clinical data were obtained from the electronic medical record, anesthesia record, and picture archiving and communication system (PACS). Baseline variables included age, sex, body mass index (BMI), involved cervical level, preoperative American Spinal Injury Association (ASIA) grade, and Hounsfield unit (HU) values of the upper and lower adjacent vertebral bodies. ASIA grading was determined according to the International Standards for Neurological Classification of Spinal Cord Injury (ISNCSCI) [13].

Perioperative variables included operative time, intraoperative blood loss, and length of hospital stay. Follow-up data included neurological recovery, cervical functional status, pain relief, radiographic outcomes, fusion status, and postoperative complications.

2.4 Surgical procedure and perioperative management

All procedures were performed under general anesthesia through a standard Smith–Robinson anterior cervical approach [14]. After fluoroscopic localization, the adjacent discs and involved vertebral body were resected, followed by direct anterior decompression under microscopic or loupe magnification. Posterior vertebral osteophytes and, when necessary, pathological portions of the posterior longitudinal ligament were removed until adequate ventral decompression was achieved. During endplate preparation, the bony endplate was preserved as much as possible and excessive curettage was avoided.

In the 3D group, a 3D-printed porous artificial vertebral body was selected according to the decompression extent and bone-defect length, packed with autologous bone, and positioned centrally within the defect. In the TMC group, the cage was trimmed to an appropriate length, shaped to fit the adjacent endplates, filled with autologous bone, and then implanted. Implant position was confirmed

fluoroscopically. In both groups, an anterior plate-and-screw construct was applied for immediate stabilization.

Postoperatively, patients received routine supportive treatment, wore a cervical brace, and underwent neurological and radiographic follow-up according to the institutional protocol.

2.5 Follow-up protocol

Radiographic examinations were performed immediately after surgery and at 6 and 12 months postoperatively. Immediate postoperative imaging was used to assess implant position and reconstructed height, whereas follow-up imaging was used to evaluate subsidence, fusion, height loss, and cervical sagittal parameters.

Fusion at 6 and 12 months was assessed using available CT scans and/or dynamic flexion–extension radiographs, with the same predefined criteria applied to both reconstruction groups and follow-up time points.

2.6 Outcome measures and definitions

Clinical outcomes included operative time, intraoperative blood loss, length of hospital stay, Japanese Orthopaedic Association (JOA) recovery rate, Neck Disability Index (NDI), and reduction in visual analogue scale (VAS) score. The JOA recovery rate was calculated using the Hirabayashi method:

JOA recovery rate = (JOA score at final follow-up − preoperative JOA score) / (17 − preoperative JOA score) × 100% [15].

The principal radiographic outcomes were:

(1) Subsidence, defined as a reduction in reconstructed segmental height of ≥ 2 mm between the immediate postoperative and final follow-up radiographs [6];

(2) Height loss (ΔH), defined as the difference between immediate postoperative and final follow-up reconstructed segmental height;

(3) Absolute change in cSVA (ΔcSVA), defined as

ΔcSVA = |cSVA_final − cSVA_immediate postoperative|;

(4) Loss of the C2–C7 Cobb angle, defined as the difference between immediate postoperative and final follow-up values; and

(5) Fusion at 6 and 12 months.

On CT, fusion was considered present when continuous trabecular bone bridging was observed across the grafted region or implant–endplate interfaces without an obvious radiolucent gap. On dynamic

radiographs, fusion was considered present when no obvious radiolucent gap was observed and only minimal segmental motion was present between flexion and extension [16, 17].

Postoperative complications included dysphagia, C5 palsy, cerebrospinal fluid leakage, fixation-related adverse events, reoperation, and severe endplate injury. Fixation-related adverse events included loosening, displacement, or breakage of the anterior plate or screws.

2.7 Radiographic measurements

All radiographic measurements were independently performed by two spine surgeons blinded to group allocation, and the mean of the two measurements was used for analysis. In cases of marked discrepancy, the images were jointly reviewed and consensus was reached.

Measurements were performed on digital images using PACS. Standardized lateral cervical radiographs were obtained in a neutral position whenever clinically feasible, and the same measurement tools and anatomical landmarks were used for each patient across postoperative and follow-up images to minimize variability related to positioning and magnification.

The measurement methods for reconstructed segmental height, C2–C7 Cobb angle, and cSVA are illustrated in Fig. 1. The cSVA was defined as the horizontal distance between a vertical plumb line from the center of C2 and the posterosuperior corner of C7. Because ΔcSVA was calculated as an absolute difference, it represented the magnitude rather than the direction of postoperative change.

HU values of the upper and lower adjacent vertebral bodies were measured on preoperative CT images. Regions of interest were placed within cancellous bone while avoiding cortical bone, fracture lines, osteophytes, and obvious sclerotic areas, and the mean HU value was recorded [5].

Interobserver agreement for continuous variables was assessed using a two-way random-effects intraclass correlation coefficient with absolute agreement [ICC(2,1)], whereas subsidence classification was assessed using Cohen's kappa. Agreement results are presented in Supplementary Table S2.

2.8 Statistical analysis

Statistical analyses were performed using SPSS version 27.0 (IBM Corp., Armonk, NY, USA) and R version 4.3.2 (R Foundation for Statistical Computing, Vienna, Austria). Continuous variables are presented as mean ± standard deviation and were compared using independent-samples t tests when normally distributed; appropriate nonparametric tests were used otherwise. Categorical variables are presented as counts and percentages and were compared using chi-square or Fisher's exact tests, as appropriate. All tests were two-sided, with $P < 0.05$ considered statistically significant.

Baseline covariate balance was additionally evaluated using standardized mean differences (SMDs), with an absolute SMD < 0.10 considered acceptable [18].

A multivariable logistic regression model was constructed with postoperative subsidence as the dependent variable. Implant type, lower adjacent vertebral HU value, age, and immediate postoperative reconstructed segmental height were included based on clinical relevance. Lower adjacent vertebral HU was scaled per 10-HU decrease, while age and immediate postoperative height were expressed per 1-year and per 1-mm increase, respectively. Odds ratios (ORs) and 95% confidence intervals (CIs) were calculated using Wald standard errors. Multicollinearity was assessed using variance inflation factors (VIFs), model discrimination using the area under the receiver operating characteristic curve (AUC), and calibration using the Hosmer–Lemeshow goodness-of-fit test.

To address measured treatment-selection imbalance, propensity scores were estimated using age, sex, BMI, upper and lower adjacent vertebral HU values, preoperative ASIA grade, and involved cervical level. Stabilized inverse probability of treatment weighting (IPTW) was applied to estimate the average treatment effect (ATE) [19]. Covariate balance before and after weighting was assessed using absolute SMDs and visualized with a Love plot (Supplementary Fig. S1). Implant type was then reassessed in the weighted cohort using weighted logistic regression with appropriate variance estimation [19].

Finally, the annual case distributions in 2023, 2024, and 2025 were compared between groups using the Pearson chi-square test to assess potential chronological imbalance (Supplementary Table S1).

3 Results

3.1 Baseline characteristics and temporal distribution

A total of 140 patients were included, with 70 patients in each group. No statistically significant between-group differences were observed in age, sex, BMI, upper or lower adjacent vertebral HU values, preoperative ASIA grade, or involved cervical level (all $P > 0.05$). However, SMDs indicated residual imbalance in several baseline covariates before weighting (Table 1).

Table 1
Comparison of baseline characteristics between the two groups

Variable	3D group (n = 70)	TMC group (n = 70)	P value	|SMD|
Age (years)	62.3 ± 2.8	61.4 ± 7.2	0.318	0.170
Male, n (%)	44 (62.9%)	52 (74.3%)	0.202	0.248
BMI (kg/m²)	26.0 ± 3.0	25.2 ± 3.1	0.105	0.276
Upper adjacent vertebral HU value	371.5 ± 75.4	390.7 ± 91.5	0.178	0.229
Lower adjacent vertebral HU value	297.7 ± 86.1	308.1 ± 69.8	0.435	0.132
Preoperative ASIA grade, n (%)			0.092	
C	15 (21.4%)	22 (31.4%)		0.228
D	35 (50.0%)	38 (54.3%)		0.086
E	20 (28.6%)	10 (14.3%)		0.354
Involved level, n (%)			0.283	
C4	21 (30.0%)	28 (40.0%)		0.211
C5	38 (54.3%)	36 (51.4%)		0.057
C6	11 (15.7%)	6 (8.6%)		0.220

Note: Data are presented as mean ± SD or n (%). SMD, standardized mean difference; BMI, body mass index; HU, Hounsfield unit; ASIA, American Spinal Injury Association; TMC, titanium mesh cage. For categorical variables with more than two levels, the P value refers to the overall chi-square comparison, whereas level-specific absolute SMDs are presented.

Both reconstruction techniques were used concurrently from 2023 to 2025, with no significant difference in annual case distribution between groups ($\chi^2 = 0.300$, P = 0.861; Supplementary Table S1). After stabilized IPTW, all measured baseline covariates achieved an absolute SMD < 0.10, with a maximum post-weighting |SMD| of 0.050 (Supplementary Fig. S1).

3.2 Perioperative and clinical outcomes

The 3D group had a shorter operative time than the TMC group (117.9 ± 12.8 vs 134.0 ± 16.0 min, P < 0.001), less intraoperative blood loss (150.1 ± 54.5 vs 179.4 ± 55.4 mL, P = 0.002), and a shorter hospital stay (7.9 ± 1.4 vs 11.3 ± 2.1 days, P < 0.001).

The JOA recovery rate was higher in the 3D group than in the TMC group (78.0 ± 13.8% vs 69.0 ± 14.3%, P < 0.001). Postoperative NDI was 18.3 ± 7.7% and 21.0 ± 8.8%, respectively, with a borderline between-

group difference (P = 0.050). Reduction in VAS score was similar between groups (4.4 ± 1.3 vs 4.3 ± 1.4, P = 0.544) (Table 2).

Table 2
Comparison of perioperative parameters and clinical outcomes between the two groups

Variable	3D group (n = 70)	TMC group (n = 70)	P value
Operative time (min)	117.9 ± 12.8	134.0 ± 16.0	< 0.001
Intraoperative blood loss (mL)	150.1 ± 54.5	179.4 ± 55.4	0.002
Length of hospital stay (days)	7.9 ± 1.4	11.3 ± 2.1	< 0.001
JOA recovery rate (%)	78.0 ± 13.8	69.0 ± 14.3	< 0.001
Postoperative NDI (%)	18.3 ± 7.7	21.0 ± 8.8	0.050
Reduction in VAS score	4.4 ± 1.3	4.3 ± 1.4	0.544

Note: Data are presented as mean ± SD. The JOA recovery rate was calculated according to the Hirabayashi method. JOA, Japanese Orthopaedic Association; NDI, Neck Disability Index; VAS, visual analogue scale; TMC, titanium mesh cage.

3.3 Radiographic outcomes

The postoperative subsidence rate was lower in the 3D group than in the TMC group (12/70 [17.1%] vs 43/70 [61.4%], P < 0.001). The 3D group also had less reconstructed segmental height loss (1.0 ± 0.6 vs 2.5 ± 0.9 mm, P < 0.001), a smaller absolute change in cSVA (11.6 ± 3.1 vs 22.0 ± 5.4 mm, P < 0.001), and less loss of the C2–C7 Cobb angle (1.0 ± 0.3° vs 3.1 ± 1.4°, P < 0.001).

At 6 months, fusion was observed in 60 of 70 patients (85.7%) in the 3D group and 28 of 70 patients (40.0%) in the TMC group (P < 0.001). At 12 months, fusion rates were 94.3% (66/70) and 88.6% (62/70), respectively, with no statistically significant between-group difference (P = 0.366) (Table 3, Fig. 4). Representative radiographic cases from the two groups are shown in Figs. 2 and 3.

Table 3
Comparison of radiographic outcomes between the two groups

Variable	3D group (n = 70)	TMC group (n = 70)	P value
Subsidence, n (%)	12 (17.1%)	43 (61.4%)	< 0.001
Height loss, ΔH (mm)	1.0 ± 0.6	2.5 ± 0.9	< 0.001
Absolute change in cSVA, ΔcSVA (mm)	11.6 ± 3.1	22.0 ± 5.4	< 0.001
Loss of C2–C7 Cobb angle (°)	1.0 ± 0.3	3.1 ± 1.4	< 0.001
Fusion at 6 months, n (%)	60 (85.7%)	28 (40.0%)	< 0.001
Fusion at 12 months, n (%)	66 (94.3%)	62 (88.6%)	0.366

Note: Subsidence was defined as a reduction in reconstructed segmental height of ≥ 2 mm between the immediate postoperative and final follow-up measurements. ΔcSVA represents the absolute change in cSVA between the immediate postoperative and final follow-up assessments. ΔH, reconstructed segmental height loss; cSVA, C2–7 sagittal vertical axis; TMC, titanium mesh cage.

Interobserver agreement was good to excellent for all continuous radiographic measurements (ICC range, 0.812–0.918), and agreement for subsidence classification was also good (Cohen's κ = 0.724; Supplementary Table S2).

3.4 Complications

Postoperative dysphagia occurred in 1 patient (1.4%) in the 3D group and 9 patients (12.9%) in the TMC group (P = 0.017). C5 palsy occurred in 0 and 3 patients, respectively (P = 0.245), and no cerebrospinal fluid leakage was observed in either group.

Fixation-related adverse events occurred in 0 patients in the 3D group and 8 patients (11.4%) in the TMC group (P = 0.006). One patient in the TMC group underwent reoperation, compared with none in the 3D group (P = 1.000). Severe endplate injury occurred in 4 patients (5.7%) and 14 patients (20.0%), respectively (P = 0.021) (Table 4). Given the small number of events in several categories, these comparisons were interpreted descriptively.

Table 4
Comparison of postoperative complications between the two groups

Variable	3D group (n = 70)	TMC group (n = 70)	P value
Dysphagia, n (%)	1 (1.4%)	9 (12.9%)	0.017
C5 palsy, n (%)	0 (0.0%)	3 (4.3%)	0.245
Cerebrospinal fluid leakage, n (%)	0 (0.0%)	0 (0.0%)	1.000
Fixation-related adverse events, n (%)	0 (0.0%)	8 (11.4%)	0.006
Reoperation, n (%)	0 (0.0%)	1 (1.4%)	1.000
Severe endplate injury, n (%)	4 (5.7%)	14 (20.0%)	0.021

Note: Data are presented as n (%). P values were calculated using Fisher's exact test because of sparse event counts in several categories. TMC, titanium mesh cage.

3.5 Multivariable logistic regression analysis of factors associated with subsidence

In the multivariable logistic regression model, use of a 3D-printed vertebral body was associated with lower odds of postoperative subsidence compared with TMC reconstruction (adjusted OR 0.035, 95% CI 0.010–0.116, P < 0.001).

Each 10-HU decrease in the lower adjacent vertebral body was associated with higher odds of subsidence (adjusted OR 1.189, 95% CI 1.096–1.291, P < 0.001). Greater immediate postoperative reconstructed segmental height was also associated with higher odds of subsidence (adjusted OR 1.417 per 1-mm increase, 95% CI 1.090–1.840, P = 0.009). Age was not significantly associated with subsidence (adjusted OR 0.979 per 1-year increase, 95% CI 0.906–1.058, P = 0.591) (Table 5, Fig. 5).

Table 5
Multivariable logistic regression analysis of factors associated with postoperative subsidence

Variable	Adjusted OR	95% CI	P value
3D-printed vertebral body (vs TMC)	0.035	0.010–0.116	< 0.001
Lower adjacent vertebral HU value (per 10-HU decrease)	1.189	1.096–1.291	< 0.001
Age (per 1-year increase)	0.979	0.906–1.058	0.591
Immediate postoperative segmental height (per 1-mm increase)	1.417	1.090–1.840	0.009

Note: Postoperative subsidence was defined as ΔH ≥ 2 mm. OR, odds ratio; CI, confidence interval; HU, Hounsfield unit; TMC, titanium mesh cage. Lower adjacent vertebral HU is expressed per 10-HU decrease. Model diagnostics were as follows: AUC = 0.884, Hosmer–Lemeshow P = 0.175, and maximum VIF = 1.12. In the stabilized IPTW sensitivity analysis, the weighted OR for the 3D group versus the TMC group was 0.078 (95% CI 0.032–0.185; P < 0.001), with a maximum post-weighting |SMD| of 0.050.

The model showed good discrimination (AUC = 0.884), with acceptable calibration (Hosmer–Lemeshow P = 0.175) and no evidence of problematic multicollinearity (maximum VIF = 1.12). In the IPTW sensitivity analysis, the association between implant type and subsidence remained directionally consistent (OR 0.078, 95% CI 0.032–0.185, P < 0.001).

4 Discussion

4.1 Principal findings and comparison with previous studies

The present study compared 3D-printed porous artificial vertebral bodies with conventional titanium mesh cages (TMCs) in patients with cervical spinal stenosis combined with hyperextension injury undergoing single-level anterior cervical corpectomy and fusion (ACCF). The main findings were that use of a 3D-printed vertebral body was associated with a lower incidence of postoperative subsidence, less reconstructed segmental height loss, a smaller absolute change in cSVA, and less loss of the C2–C7 Cobb angle. In addition, the 6-month fusion rate was substantially higher in the 3D group, whereas the difference in fusion rate was no longer statistically significant at 12 months. The association between implant type and subsidence remained directionally consistent after multivariable adjustment and IPTW sensitivity analysis. Nevertheless, because treatment allocation was nonrandomized, these findings should be interpreted as associations rather than causal treatment effects.

These results are broadly consistent with previous comparative evidence. Meta-analytic and comparative studies have suggested that 3D-printed vertebral bodies may be associated with lower subsidence, improved maintenance of reconstructed vertebral height, and favorable cervical sagittal parameters, whereas differences in functional outcomes have been less consistent [9–12]. A previous

propensity score-matched analysis similarly indicated that the main differences between artificial vertebral bodies and TMCs may be reflected in early fusion and radiographic maintenance rather than in mid-term clinical recovery [11]. Zhang et al. [20] also reported favorable perioperative and radiographic findings with 3D-printed titanium vertebral bodies in patients with cervical spondylotic myelopathy.

The present study extends these observations to patients with pre-existing cervical stenosis complicated by hyperextension injury. In this population, traumatic neurological injury occurs on a background of degenerative canal narrowing, making both adequate decompression and reliable anterior column reconstruction important. Of particular interest, the marked difference in fusion at 6 months was no longer evident at 12 months. This pattern suggests that the potential advantage of the 3D-printed implant may relate primarily to accelerated early fusion rather than a substantially greater ultimate probability of fusion. Thus, the observed differences should not be interpreted as evidence that the 3D-printed implant is universally preferable to TMC reconstruction.

4.2 Interface stability, bone quality, and reconstruction height

Subsidence after ACCF is influenced by implant–endplate contact, load transmission, endplate integrity, reconstruction height, and bone quality. Conventional TMCs provide reliable structural support but generally require intraoperative trimming and adaptation. Limited conformity between the cage and vertebral endplates may result in localized stress concentration, particularly when the endplate is weakened or bone quality is poor [4, 6]. In contrast, 3D-printed porous vertebral bodies may provide a larger contact area, improved endplate conformity, and a porous surface favorable for initial stability and bone ingrowth [8, 9]. These characteristics provide a plausible explanation for the radiographic differences observed in the present study, although the underlying biomechanical mechanisms were not directly measured.

After adjustment for age, lower adjacent vertebral HU value, and immediate postoperative segmental height, implant type remained associated with postoperative subsidence. A similar direction of association was observed after IPTW. However, the magnitude of this association was considerable, and unmeasured factors such as endplate preparation, distraction, implant fitting, surgeon preference, and other technical variables may still have contributed. The regression results should therefore be interpreted as evidence of an association within the measured dataset rather than proof that implant type alone determines subsidence.

Immediate postoperative reconstructed height was also associated with subsidence. Greater distraction may restore segmental height and facilitate decompression, but excessive distraction can increase endplate loading and has previously been associated with postoperative subsidence after ACCF [6, 21]. Bone quality was another relevant factor. Each 10-HU decrease in the lower adjacent vertebral body was associated with higher odds of subsidence. CT-derived HU values have increasingly been used for opportunistic assessment of cervical bone quality and have been associated with subsidence after anterior cervical reconstruction [5, 22, 23]. Other measures, including peripheral bone mineral density

and endplate-specific HU values, may further refine risk assessment [24–26]. These observations support considering implant geometry, endplate integrity, reconstruction height, and bone quality together when planning anterior column reconstruction.

4.3 Clinical outcomes, perioperative findings, and complications

The clinical findings should be interpreted more cautiously than the radiographic outcomes. The JOA recovery rate was higher in the 3D group, whereas VAS improvement was similar and the between-group difference in postoperative NDI was borderline. In addition, baseline neurological status showed some imbalance before weighting. Therefore, the difference in JOA recovery cannot be attributed directly to implant type. Neurological recovery after cervical hyperextension injury is influenced by the initial severity of spinal cord injury, adequacy and timing of decompression, baseline neurological status, age, and rehabilitation. Although stable reconstruction may theoretically contribute to a favorable recovery environment, the present study cannot establish this mechanism.

The 3D group also had shorter operative time, less intraoperative blood loss, and a shorter hospital stay. A preformed vertebral body may reduce the need for repeated trimming and trial placement compared with a conventional TMC [8, 20]. However, these perioperative differences may also have been influenced by surgeon experience, workflow, case complexity, and other unmeasured factors. Both implants were used concurrently during 2023–2025, and their annual distributions were similar, which reduces concern that the findings merely reflect sequential replacement of one implant by another. Nevertheless, residual learning-curve and chronological effects cannot be fully excluded.

Dysphagia, fixation-related adverse events, and severe endplate injury were more frequent in the TMC group. However, the number of events was small, and these findings should therefore be interpreted descriptively. Dysphagia after anterior cervical surgery is multifactorial and may be influenced by operative duration, soft-tissue retraction, surgical exposure, and patient characteristics [27]. Similarly, fixation-related events and endplate injury may reflect not only implant characteristics but also endplate preparation, distraction, placement accuracy, and surgical technique. Larger studies with more complication events are needed before firm conclusions regarding comparative complication risk can be drawn.

4.4 Limitations and future directions

Several limitations should be acknowledged. First, this was a single-center retrospective study with nonrandomized implant selection. Treatment choice was influenced partly by patient preference and financial considerations because the 3D-printed implant was more expensive than conventional TMC. Socioeconomic factors were not quantitatively recorded, and residual treatment-selection bias therefore remains possible. Although IPTW substantially improved balance in measured baseline covariates, weighting cannot eliminate confounding from unmeasured variables.

Second, several technical factors potentially related to subsidence were not fully captured, including the extent of endplate preparation, intraoperative distraction, implant–endplate conformity, detailed endplate morphology, and surgeon-specific technique. Third, although both reconstruction methods were used concurrently and their yearly distributions were similar, changes in surgeon experience and perioperative management over time cannot be completely excluded. Fourth, fusion was assessed using available CT scans and/or dynamic flexion–extension radiographs rather than a uniform imaging modality in every patient. Although predefined criteria were applied consistently, this may have introduced some assessment heterogeneity.

Fifth, ΔcSVA represented the absolute difference between immediate postoperative and final follow-up measurements. It therefore reflects the magnitude of change but not its direction, and a smaller ΔcSVA should not be interpreted as unequivocal evidence of better directional sagittal alignment. Finally, the sample size limited the precision of analyses of uncommon complications, and the main follow-up duration of 12 months was insufficient to evaluate long-term reconstruction durability, adjacent-segment changes, or delayed complications.

Future multicenter prospective studies with larger samples and longer follow-up should incorporate detailed measures of bone quality, endplate morphology, reconstruction height, implant–endplate matching, and surgeon-related technical factors. Such studies may clarify whether the observed differences in early fusion and subsidence translate into sustained functional or radiographic benefits.

5 Conclusions

In patients with cervical spinal stenosis combined with hyperextension injury undergoing single-level ACCF, reconstruction with a 3D-printed porous artificial vertebral body was associated with a lower incidence of postoperative subsidence, less loss of reconstructed segmental height, a smaller absolute change in cSVA, and a higher early fusion rate than conventional TMC reconstruction. The between-group difference in fusion was no longer significant at 12 months, suggesting that the potential benefit of the 3D-printed implant may lie primarily in accelerating early fusion rather than increasing the ultimate likelihood of fusion. Lower HU values of the lower adjacent vertebral body and greater immediate postoperative reconstructed height were also associated with higher odds of subsidence. These findings support the importance of bone-quality assessment and appropriate reconstruction height in ACCF planning. However, because of the retrospective nonrandomized design, residual treatment-selection bias and unmeasured confounding cannot be excluded, and prospective multicenter studies are needed for further validation.

Abbreviations

ACCF
Anterior cervical corpectomy and fusion
ASIA

American Spinal Injury Association
ATE
Average treatment effect
AUC
Area under the receiver operating characteristic curve
BMI
Body mass index
CI
Confidence interval
CT
Computed tomography
cSVA
C2–7 sagittal vertical axis
HU
Hounsfield unit
ICC
Intraclass correlation coefficient
IPTW
Inverse probability of treatment weighting
ISNCSCI
International Standards for Neurological Classification of Spinal Cord Injury
JOA
Japanese Orthopaedic Association
MRI
Magnetic resonance imaging
NDI
Neck Disability Index
OPLL
Ossification of the posterior longitudinal ligament
OR
Odds ratio
PACS
Picture archiving and communication system
SD
Standard deviation
SMD
Standardized mean difference
TMC
Titanium mesh cage
VAS

Visual analogue scale
VBQ
Vertebral bone quality
VIF
Variance inflation factor
ΔcSVA
Absolute change in C2–7 sagittal vertical axis
ΔH
Reconstructed segmental height loss

Declarations

Clinical trial number

Not applicable.

Ethics approval and consent to participate

This retrospective study was conducted in accordance with the ethical standards of the institutional and/or national research committee and with the 1964 Declaration of Helsinki and its later amendments. The study protocol was reviewed and approved by the Ethics Committee of the Qilu Hospital of Shandong University (Approval No. QLCR20260629). Given the retrospective design and the use of anonymized clinical data, the requirement for written informed consent was waived by the Ethics Committee of the Qilu Hospital of Shandong University in accordance with relevant national regulations. No oral consent was required according to the institutional ethical policy.

Consent for publication

Not applicable. This study was a retrospective analysis using anonymized clinical data, and no individual patient-identifiable information is included in this publication.

Funding

This research did not receive any specific grant from funding agencies in the public, commercial, or not-for-profit sectors.

Author Contribution

Linyang Song and Xin Xu contributed equally to this work. Xin Xu, Linyang Song, and Guangjun Jiao designed the study. Linyang Song collected the clinical and imaging data. Linyang Song and Xin Xu performed the statistical analyses and drafted the manuscript. Linyang Song, Xin Xu, and Guangjun Jiao

participated in imaging review and data verification. Linyang Song and Xin Xu contributed to clinical data management, figure preparation, and manuscript organization. Guangjun Jiao supervised the study, critically revised the manuscript, and approved the final version for submission. All authors read and approved the final manuscript.

Acknowledgement

The authors thank the medical and nursing staff of the Department of Spine Surgery, Qilu Hospital of Shandong University, for their support in patient care and data collection.

Data Availability

The datasets generated and/or analyzed during the current study are not publicly available due to institutional regulations regarding patient data confidentiality, but are available from the corresponding author on reasonable request.

References

1. Carr MT, Harrop JS, Houten JK. Traumatic central cord syndrome. Clin Spine Surg. 2024;37(9):379–87.
2. Park S, Lee DH, Lee CS, Hwang CJ, Yang JJ, Cho JH. Anterior decompression and fusion for the treatment of cervical myelopathy caused by ossification of the posterior longitudinal ligament: a narrative review. Asian Spine J. 2023;17(3):582–94.
3. Sun N, Jiang C, Liu Y. Surgical options for ossification of the posterior longitudinal ligament of the cervical spine: a narrative review. J Orthop Surg Res. 2024;19(1):707.
4. Dhar UK, Menzer EL, Lin M, Hagerty V, O'Connor T, Tsai CT, et al. Factors influencing cage subsidence in anterior cervical corpectomy and discectomy: a systematic review. Eur Spine J. 2023;32(3):957–68.
5. Wang Z, Mei J, Feng X, Deng C, Tian X, Lv J, et al. Low cervical vertebral CT value increased early subsidence of titanium mesh cage after anterior cervical corpectomy and fusion. J Orthop Surg Res. 2022;17(1):355.
6. Tang Y, Geng X, Li F, Sun Y, Jia L, Zhou S, et al. Factors affecting titanium mesh cage subsidence in single-level anterior cervical corpectomy and fusion for ossification of the posterior longitudinal ligament. BMC Musculoskelet Disord. 2022;23(1):1092.
7. Wang S, Yang H, Liao H, et al. MRI-based cervical VBQ scores as predictors of cage subsidence in cervical spine surgery: a meta-analysis. Global Spine J. 2025;15(7). 10.1177/21925682251327381.
8. Lewandrowski KU, Vira S, Elfar JC, Lorio MP. Advancements in custom 3D-printed titanium interbody spinal fusion cages and their relevance in personalized spine care. J Pers Med. 2024;14(8):809.

9. Cheng H, Luo G, Xu D, Li Y, Wang Z, Yang H, et al. Comparison of radiological and clinical outcomes of 3D-printed artificial vertebral body with titanium mesh cage in single-level anterior cervical corpectomy and fusion: a meta-analysis. Front Surg. 2023;9:1077551.
10. He H, Fan L, Lü G, et al. Myth or fact: 3D-printed off-the-shelf prosthesis is superior to titanium mesh cage in anterior cervical corpectomy and fusion? BMC Musculoskelet Disord. 2024;25(1):96.
11. Wang H, Qu R, Xia T, et al. Artificial vertebral body versus titanium mesh cage for single-level anterior cervical corpectomy and fusion (ACCF): a propensity score matching analysis of fusion, implant subsidence and clinical outcomes. BMC Musculoskelet Disord. 2025;26:1060.
12. Li J, Zhang J, Wang B, et al. Comparison of titanium mesh cage, nano-hydroxyapatite/polyamide cage, and three-dimensional-printed vertebral body for anterior cervical corpectomy and fusion. Spine (Phila Pa 1976). 2025;50(2):88–95.
13. Rupp R, Biering-Sørensen F, Burns SP, et al. International Standards for Neurological Classification of Spinal Cord Injury: revised 2019. Top Spinal Cord Inj Rehabil. 2021;27(2):1–22.
14. Vigo V, Franzini A, Costa F, et al. The Smith-Robinson approach to the subaxial cervical spine: a stepwise microsurgical technique using volumetric models from anatomic dissections. World Neurosurg. 2020;141:413–22.
15. Oshima Y, Seichi A, Takeshita K, et al. Comparison between the Japanese Orthopaedic Association score and modified Japanese Orthopaedic Association score for evaluating cervical myelopathy as a patient-reported outcome measure. Global Spine J. 2022;12(5):795–800.
16. Oshina M, Oshima Y, Tanaka S, et al. Radiological fusion criteria of postoperative anterior cervical discectomy and fusion: a systematic review. Global Spine J. 2018;8(7):739–50.
17. Wang H, Xia T, Qu R, et al. Interspinous motion measurement could serve as a quantitative method for assessing bony fusion after anterior cervical corpectomy and fusion. Spine (Phila Pa 1976). 2025;50(3):E39–45.
18. Austin PC. Balance diagnostics for comparing the distribution of baseline covariates between treatment groups in propensity-score matched samples. Stat Med. 2009;28(25):3083–107. 10.1002/sim.3697.
19. Austin PC, Stuart EA. Moving towards best practice when using inverse probability of treatment weighting (IPTW) using the propensity score to estimate causal treatment effects in observational studies. Stat Med. 2015;34(28):3661–79. 10.1002/sim.6607.
20. Zhang G, Zhang T, Zhang X, Guo Y, Fan L, Cheng B, et al. 3D-printed titanium vertebra in the treatment of cervical spondylotic myelopathy: a comparative analysis of perioperative, radiographic, and clinical outcomes. J Orthop. 2025;65:283–9.
21. Qu R, Wang H, Xia T, et al. Risk factors of early subsidence of 3D-printed artificial vertebral body following single-level anterior cervical corpectomy and fusion (ACCF): retrospective study of 98 patients. J Orthop Surg Res. 2025;20(1):633.
22. Lo Bu R, Fluss R, Srivastava Y, De la Garza Ramos R, Murthy SG, Yassari R, et al. Hounsfield unit utilization in cervical spine for bone quality assessment: a scoping review. J Clin Med.

2025;14(2):442.
23. Abudouaini H, Wu T, Liu H, Wang B, Chen H. The predictive value of Hounsfield units for titanium mesh cage subsidence after anterior cervical corpectomy and fusion. Front Surg. 2022;9:1012364.
24. Wang J, Wang J, Liu X, et al. Forearm bone mineral density predicts subsidence of titanium mesh cage after anterior cervical corpectomy and fusion in patients with cervical spondylosis. J Orthop Surg Res. 2025;20(1):436.
25. Levy HA, Astudillo Potes MD, Messer CJ, Magera CA, Wodajo FM, Elder BD, et al. The superiority of endplate Hounsfield units relative to cervical vertebral Hounsfield units in predicting subsidence after anterior cervical discectomy and fusion. J Neurosurg Spine. 2025;43(6):672–80.
26. Pinter ZW, Reed R, Townsley SE, Mikula AL, Dittman L, Xiong A, et al. Titanium cervical cage subsidence: postoperative computed tomography analysis defining incidence and associated risk factors. Global Spine J. 2023;13(7):1703–15.
27. Katsikas A, Georgountzos G, Stamatopoulou A, Gkalonakis I, Tsitsopoulos P, Paleologos T, et al. Complications associated with anterior cervical spine surgery: a systematic review of literature. Brain Spine. 2025;6:105897.

Figures

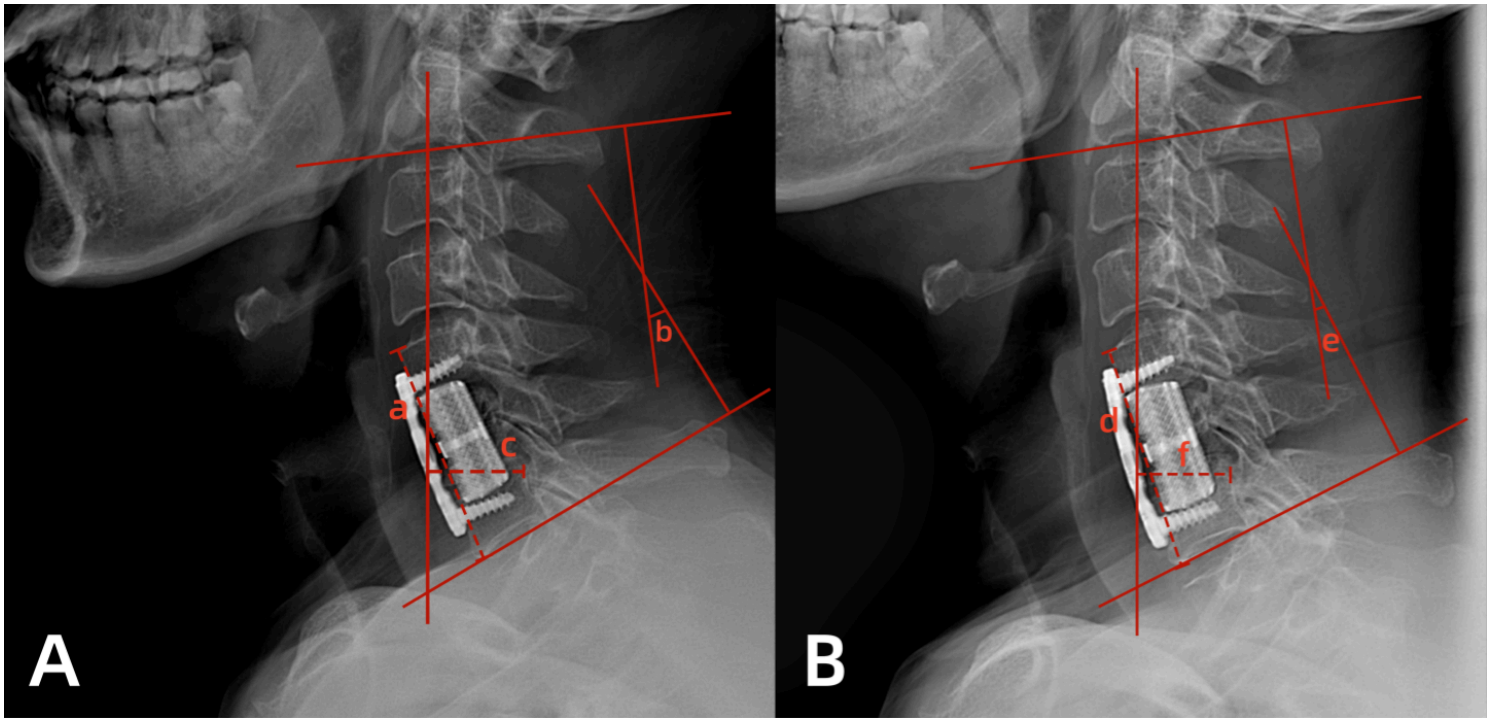


Figure 1

Radiographic measurement schematic

(A) Immediate postoperative lateral radiograph. a indicates the immediate postoperative reconstructed segmental height, b the immediate postoperative C2–C7 Cobb angle, and c the immediate postoperative

C2–7 sagittal vertical axis (cSVA).
(B) Final follow-up lateral radiograph. d indicates the reconstructed segmental height at final follow-up, e the C2–C7 Cobb angle at final follow-up, and f the cSVA at final follow-up. Height loss (ΔH), loss of the C2–C7 Cobb angle, and the absolute change in cSVA were calculated from the corresponding immediate postoperative and final follow-up measurements. ΔcSVA = |f − c|.

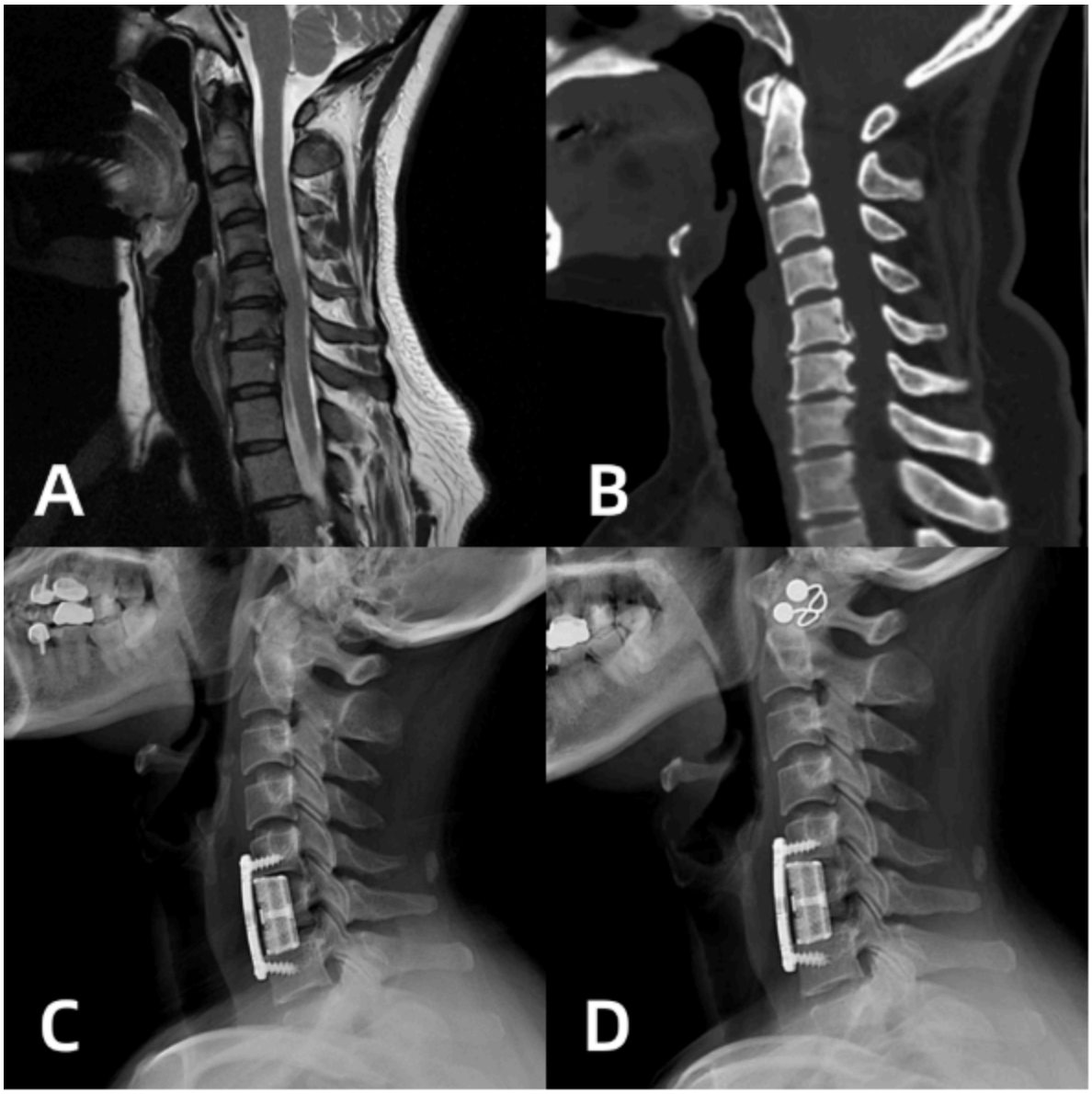


Figure 2

Representative imaging findings of reconstruction with a 3D-printed porous artificial vertebral body.

(A) Preoperative sagittal MRI showing spinal cord compression at the involved segment.
(B) Preoperative sagittal CT showing spinal canal stenosis and anterior bony compression at the involved segment.
(C) Immediate postoperative lateral radiograph showing implantation of a 3D-printed porous artificial vertebral body with anterior plate fixation after single-level ACCF, with satisfactory implant position.

(D) Lateral radiograph obtained 12 months postoperatively showing stable internal fixation and bony fusion of the reconstructed segment.

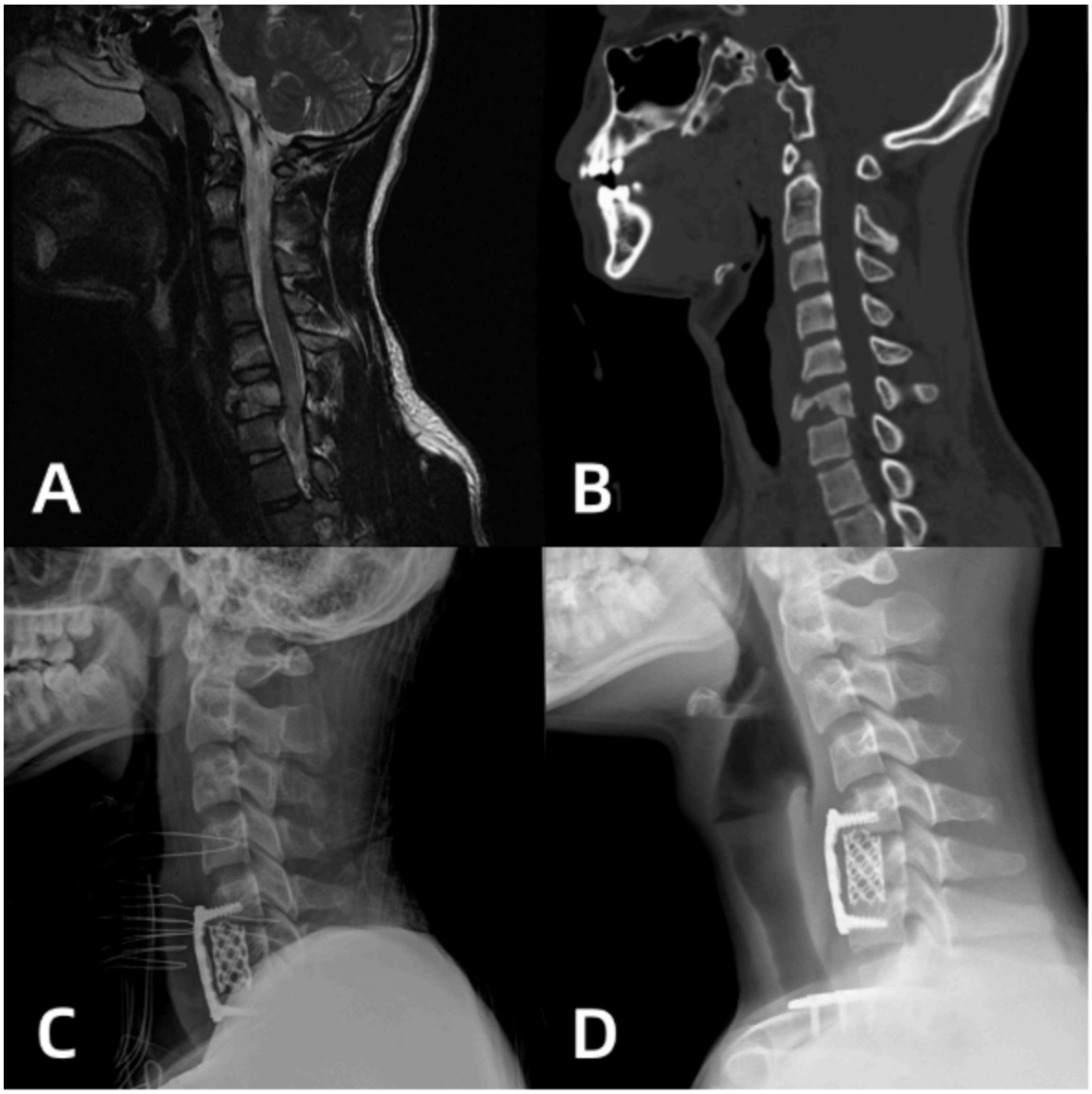


Figure 3

Representative imaging findings of reconstruction with a titanium mesh cage (TMC).

(A) Preoperative sagittal MRI showing spinal cord compression at the involved segment.
(B) Preoperative sagittal CT showing spinal canal stenosis and anterior bony compression at the involved segment.
(C) Immediate postoperative lateral radiograph showing TMC implantation with anterior plate fixation after single-level ACCF, with satisfactory implant position.
(D) Lateral radiograph obtained 12 months postoperatively showing stable internal fixation and bony fusion of the reconstructed segment.

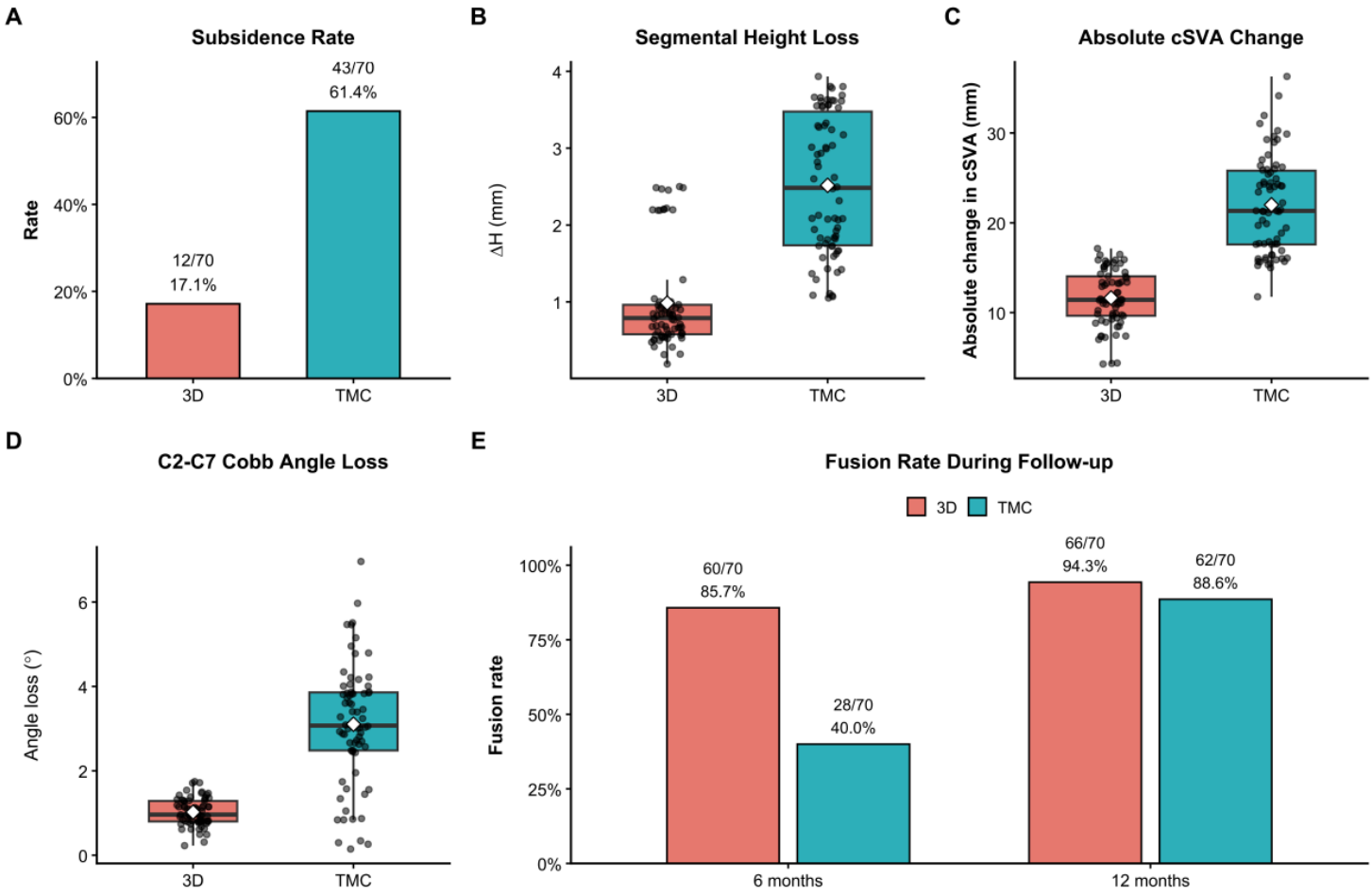


Figure 4

Comparison of the main radiographic outcomes between the two groups.

(A) Postoperative subsidence rate.
(B) Reconstructed segmental height loss (ΔH).
(C) Absolute change in C2–7 sagittal vertical axis (ΔcSVA).
(D) Loss of the C2–C7 Cobb angle.
(E) Fusion rates at 6 and 12 months postoperatively.

Data are presented for the 3D-printed vertebral body group and the titanium mesh cage (TMC) group. Individual observations are shown for continuous radiographic outcomes where applicable.

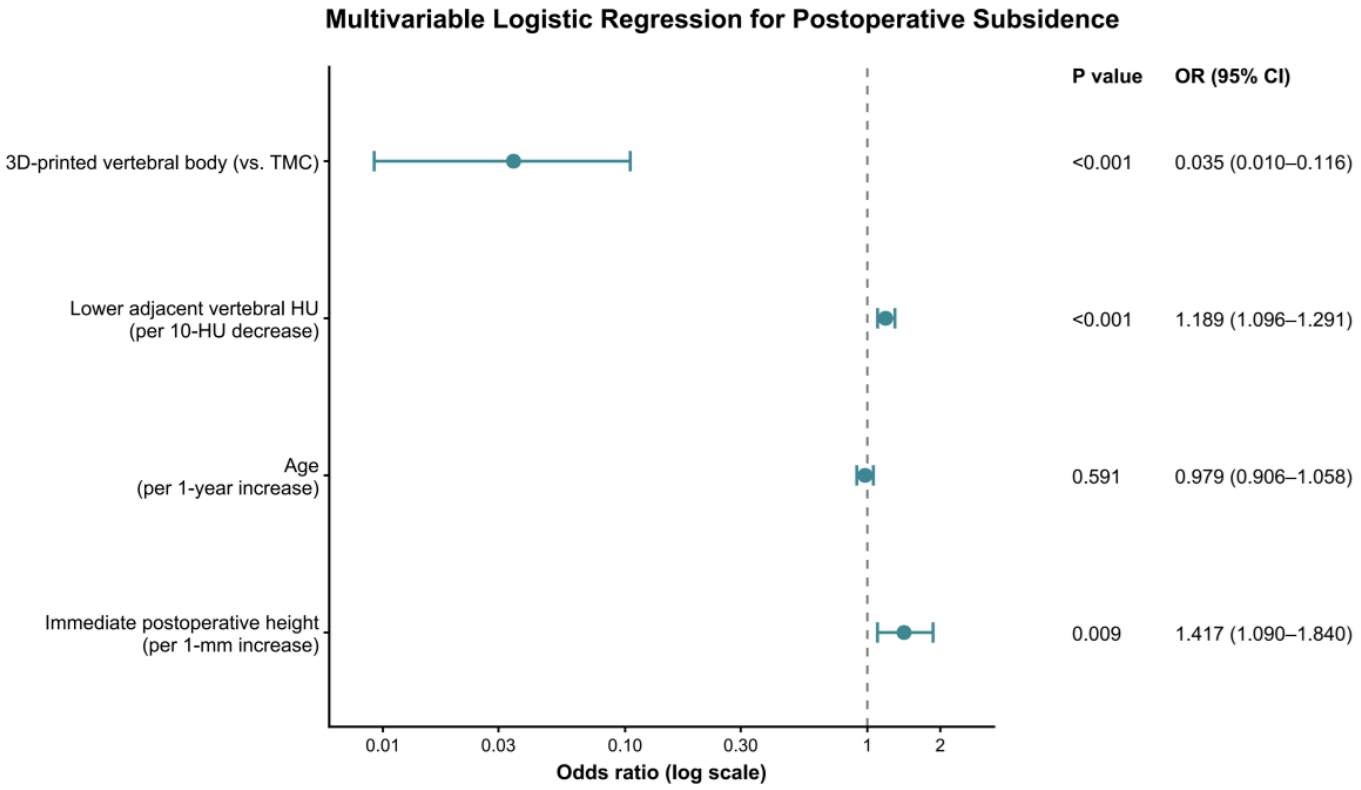


Figure 5

Multivariable logistic regression analysis of factors associated with postoperative subsidence.

Adjusted odds ratios (ORs) and 95% confidence intervals (CIs) are shown for implant type, lower adjacent vertebral HU value, age, and immediate postoperative reconstructed segmental height. Lower adjacent vertebral HU is expressed per 10-HU decrease, age per 1-year increase, and immediate postoperative height per 1-mm increase. The vertical dashed line indicates OR = 1. TMC, titanium mesh cage; HU, Hounsfield unit.

Supplementary Files

This is a list of supplementary files associated with this preprint. Click to download.

- SupplementaryTableS2.docx
- SupplementaryTableS1.docx
- SupplementaryFigureS1.png